Bioorganic & Medicinal Chemistry Letters 26 (2016) 4613–4619

Contents lists available at ScienceDirect

Bioorganic & Medicinal Chemistry Letters

journal homepage: www.elsevier.com/locate/bmcl

Dual action Smac mimetics–zinc chelators as pro-apoptotic antitumoral agents

Leonardo Manzoni [a], Davide Gornati [c], Mattia Manzotti [c], Silvia Cairati [a], Alberto Bossi [a,b], Daniela Arosio [a,b], Daniele Lecis [d], Pierfausto Seneci [c,*]

[a] Istituto di Scienze e Tecnologie Molecolari (ISTM), Consiglio Nazionale delle Ricerche (CNR), Via Golgi 19, I-20133 Milan, Italy
[b] SmartMatLab, Centre, Via Golgi 19, I-20133 Milan, Italy
[c] Dipartimento di Chimica, Università degli Studi di Milano, Via Golgi 19, I-20133 Milan, Italy
[d] Dipartimento di Oncologia Sperimentale e Medicina Molecolare, Fondazione IRCCS Istituto Nazionale Tumori, Via Amadeo 42, I-20133 Milan, Italy

ARTICLE INFO

Article history:
Received 27 June 2016
Revised 18 August 2016
Accepted 20 August 2016
Available online 22 August 2016

Keywords:
Dual action compounds
Smac mimetics
Zinc chelation
Apoptosis
Peptidomimetics

ABSTRACT

Dual action compounds (DACs) based on 4-substituted aza-bicyclo[5.3.0]decane Smac mimetic scaffolds (ABDs) linked to a Zn^{2+}-chelating moiety (DPA, *o*-hydroxy, *m*-allyl, *N*-acyl (*E*)-phenylhydrazone) through their 10 position are reported and characterized. Their synthesis, their target affinity (XIAP BIR3, Zn^{2+}) in cell-free assays, their pro-apoptotic effects and cytotoxicity in tumor cells with varying sensitivity to Smac mimetics are described. The results are interpreted to evaluate the influence of Zn^{2+} chelators on cell-free potency and on cellular permeability of DACs, and to propose novel avenues towards more potent antitumoral DACs based on Smac mimetics and Zn^{2+} chelation.

Cancer implies a variety of pathologically altered mechanisms, and hundreds of putative molecular targets.[1] Tumor cells become resistant to candidates either by mutating their target (i.e., imatinib[2]), or by effluxing them outside the cancer cell (i.e., taxol[3]). A *dual action compound* (*DAC*) interferes with two validated cancer targets, and should overcome resistance. We reported[4] integrin antagonist-Smac mimetic DACs, exploiting our experience with anti-angiogenetic[5] and pro-apoptotic[6] agents.

Zinc is involved in the catalytic function and structural stability of over 300 enzymes and proteins.[7] Zinc ions prevent the autocatalytic conversion of procaspase-3 to active caspase-3 by interaction with its 'safety catch' DDD sequence.[8] Zinc chelation/depletion induces rapid degradation of inhibitor of apoptosis proteins (IAPs) via activation of caspase-3 and -9 in PC-3 cells.[9]

Smac-DIABLO is a mitochondrial protein that binds to IAPs,[10] frees apoptosis-related caspases-3, -7 and -9,[11] induces degradation of cellular IAPs (cIAPs),[12] and restores apoptosis in cancer cells. Substituted aza-bicyclo[5.3.0]decane derivatives (ABDs) are potent, cytotoxic Smac mimetics targeted against IAPs.[6,13] We reasoned that zinc depletion by Zn^{2+}-chelating DACs built around ABDs should activate caspases and restore apoptosis in cancer cells.

Benzoylated 4-alkylamine ABDs **1** and **2** are potent, cell permeable pro-apoptotic leads (Fig. 1).[6] Their 10-benzhydrylamide substituent is essential for IAP binding through its pro-(*S*) phenyl group.[13] We replaced the IAP binding-irrelevant pro-(*R*)-phenyl group with a Zn^{2+}-chelating moiety.

Our synthetic strategy required access to multi-gram quantities of *N*-Boc-protected 10-carboxy ABDs **3** and **4** (Fig. 1). We optimized their synthesis by improving yields, reducing side reactions and simplifying experimental protocols. Scheme 1 reports the 10-step, optimized synthesis of compound **3**. Its ≈50% yield is a significant increase with respect to published un-optimized routes to **3**.[6,14] Similar improvements were obtained also within the synthetic route to compound **4**.[15]

The Zn^{2+} K_d of known polypyridyl Zn^{2+} chelators[16] varies between nano- (tri-dentate 2,2′-dipicolylamine, DPA, **5**) and femtomolar values (hexa-dentate *N*,*N*,*N*′,*N*′,-tetrakis(2-pyridylmethyl) ethylenediamine, TPEN, **6**, Fig. 2). We reasoned that a small, nanomolar Zn^{2+} chelating moiety coupled to a potent Smac mimetic should ensure Zn^{2+} chelation in the vicinity of caspases and IAPs. A DPA-like moiety should also reduce the risk of aspecific Zn^{2+} chelation elsewhere, and should limit the molecular weight of the resulting DACs.

We selected three DPA-based reagents to be coupled with the 10-COOH group of compound **3**. DPA itself was coupled to **3** by

* Corresponding author. Tel.: +39 0250314060.
E-mail address: pierfausto.seneci@unimi.it (P. Seneci).

http://dx.doi.org/10.1016/j.bmcl.2016.08.065
0960-894X/

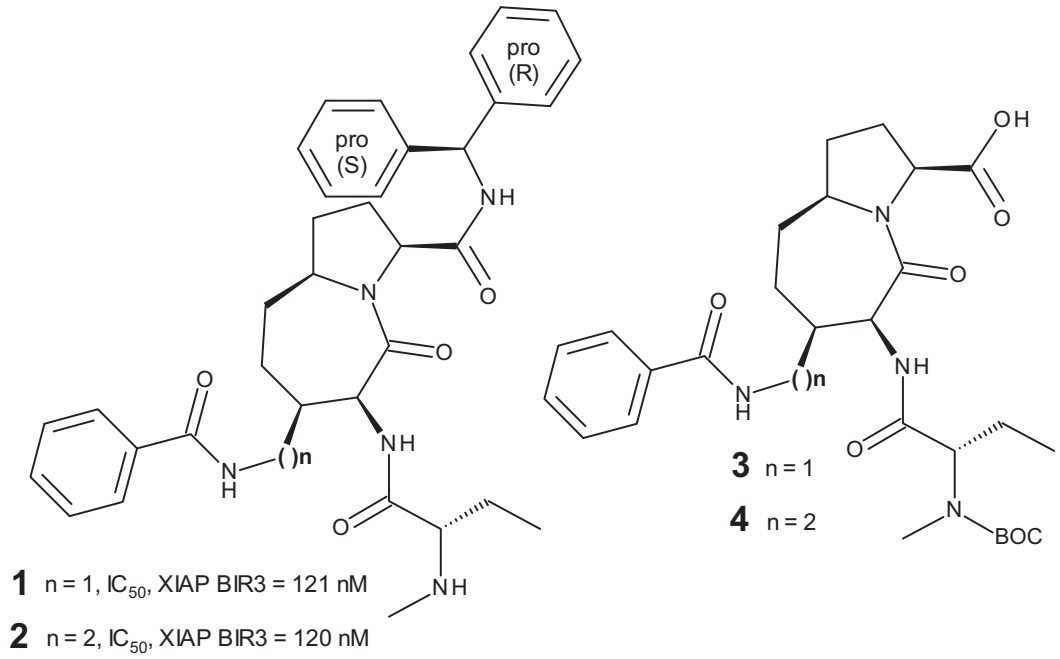

Figure 1. Structure of pro-apoptotic Smac mimetics **1** and **2**, and of key synthetic intermediates **3** and **4**.

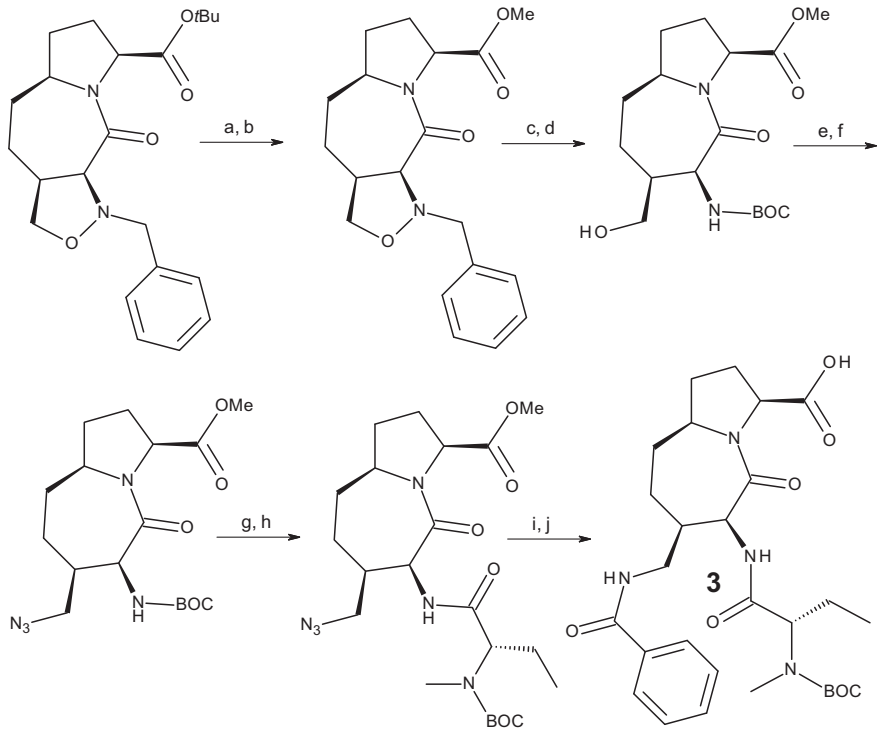

a, TFA, Et_3SiH, CH_2Cl_2, rt; b, $SOCl_2$, MeOH, 0°C to rt, **98%** (2 steps); c, H_2, Pd/C, EtOH/H_2O 85/15, 0.7 mL/min, 85°C, 10 bar; d, Boc_2O, TEA, CH_2Cl_2, rt, **77%** (2 steps); e, MsCl, TEA, CH_2Cl_2, rt; f, NaN_3, DMF, 80°C, **95%** (2 steps); g, TFA, DCM, rt; h, N-Me,N-Boc-(S)-2-aminobutyric acid, TBTU, HOBt, DIPEA, CH_2Cl_2/DMF 8/1, rt, **81%** (2 steps); i, Me_3P, PhCOOH, PyS-SPy, toluene, 0° to 55°C; j, LiOH, THF/H_2O 3/1, rt, **88%** (2 steps).

Scheme 1. Synthesis of key intermediate **3**.

means of standard peptide coupling conditions (Scheme 2). The synthesized 'negative control' amide **8** does not contain the 10 (*S*)-phenyl group, and should lose the chelation ability of its tridentate DPA moiety due to amide bond formation.[17]

DPA was condensed with *N*-Boc (*S*)-phenylglycine **9**, and after N-deprotection the amine **11** was coupled to **3** in standard peptide coupling conditions (Scheme 3, steps a–c).[18] The resulting amide **13** contains a 10 (*S*) phenyl group, that should ensure IAP

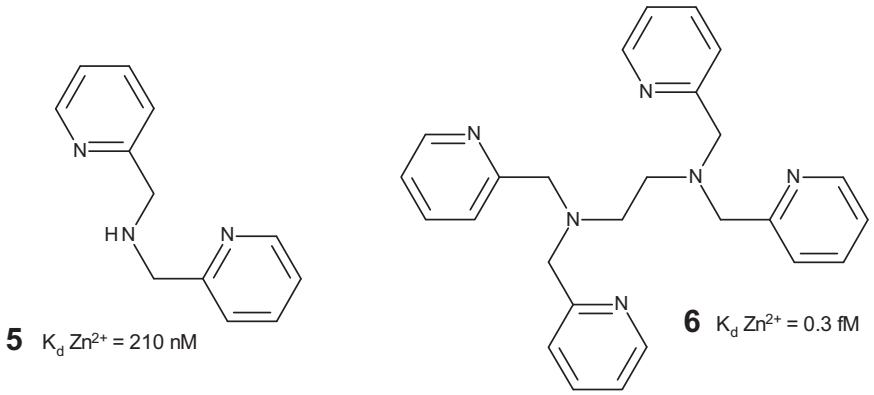

Figure 2. Structure of polypyridyl Zn^{2+} chelating agents **5** (DPA) and **6** (TPEN).

binding/inhibition. The chelation ability of its tridentate DPA moiety should still be inactivated by the amide bond.

The HPLC chromatogram of *N*-protected amide **12** showed two close, equimolar peaks with the expected MW. We attributed them to racemization of *N*-Boc (*S*)-phenylglycine **9** during its coupling with DPA (step a). Reverse phase purification after N-deprotection produced two batches of diastereomers **13a** and **13b**, each with >90% diastereomeric excess (Scheme 3).

A revised experimental protocol based on mixed anhydride coupling between DPA and *N*-Boc (*S*)-phenylglycine **9** (steps a′, a″), lower reaction temperature and hindered *sym*-collidine as a base (step c′, Scheme 3) was set up after extensive optimization. It produced a strongly enriched batch of 10 (*S*)-diastereomer **13a** (92% de).

N,*N*,-Bis(2-pyridylmethyl)ethylenediamine **14** (BPEN)[19] was condensed with *N*-Boc (*S*)-phenylglycine, and after N-deprotection amine **16** was coupled to **3** in standard peptide coupling conditions (Scheme 4). The resulting amide **18** contains a 10 (*S*)-phenyl group, that should ensure IAP binding/inhibition. The inserted ethylenediamine spacer should preserve the chelation ability of its tridentate DPA moiety. Thus, **18** should be a Smac mimetic—Zn^{2+} chelator DAC (DAC–DPA).[17]

We observed by HPLC two equimolar diastereomeric DACs **18a**, **b**, most likely due to *N*-Boc (*S*)-phenylglycine racemization during its coupling with BPEN, as observed during *N*-Boc (*S*)-phenylglycine coupling with DPA in the synthesis of **13a**,**b**. Reverse phase purification produced two batches of pure **18a** and **18b**, with >90% diastereomeric excess (Scheme 4). We will verify the effectiveness of optimized experimental conditions (steps a′, a″, Scheme 3) to synthesize a strongly enriched batch of 10 (*S*) diastereomer **18a**.

PAC-1 (procaspase activating compound 1, **19**, Fig. 3) was identified as a procaspase 3 activator in a HTS campaign.[20] The *o*-hydroxy, *m*-allyl, *N*-acyl (*E*)-phenylhydrazone moiety in PAC-1 activates caspase 3 by chelation of procaspase-bound Zn^{2+}.[21] We synthesized a PAC-1-based DAC **20** (DAC–PAC-1), bridging the *o*-hydroxy, *m*-allyl, *N*-acyl (*E*)-phenylhydrazone moiety with the 10 COOH group of Smac mimetic **4** (Scheme 5).[17]

The *N*-Boc protecting group in compound **9** was converted to *N*-Teoc (steps a, b, compound **21**) to prevent acid degradation of PAC-1-like acylhydrazones. The *o*-hydroxy, *m*-allyl, *N*-acyl (*E*)-phenylhydrazone moiety was built in a two step sequence (steps c and d), using conditions known to minimize epimerization and to decrease the formation of the unwanted (*Z*)-hydrazone. Teoc deprotection (step e) gave the aminoacyl hydrazone **22**. The Smac mimetic **4** was *N*-deprotected (step f, compound **23**), to avoid an acylhydrazone-harmful acid deprotection. Coupling of **23** with **22** (step g, Scheme 5) provided, after purification, enantiomerically pure DAC **20** in moderate yield.

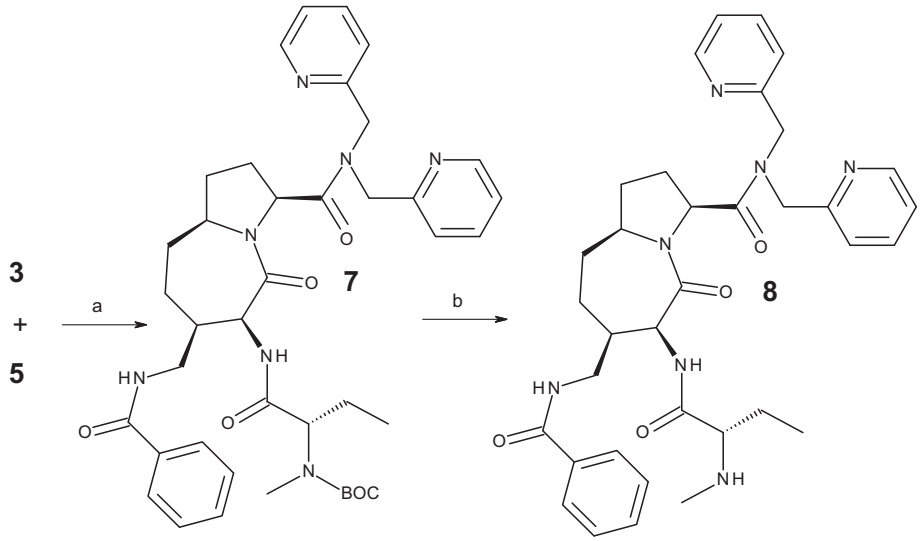

a, HBTU, HOBt, dry DIPEA, dry CH_2Cl_2/DMF 8/1, N_2, rt, **85%**;
b, TFA, CH_2Cl_2, 0°C to rt, reverse phase HPLC, **87%**.

Scheme 2. Synthesis of 'negative control' DPA amide **8**.

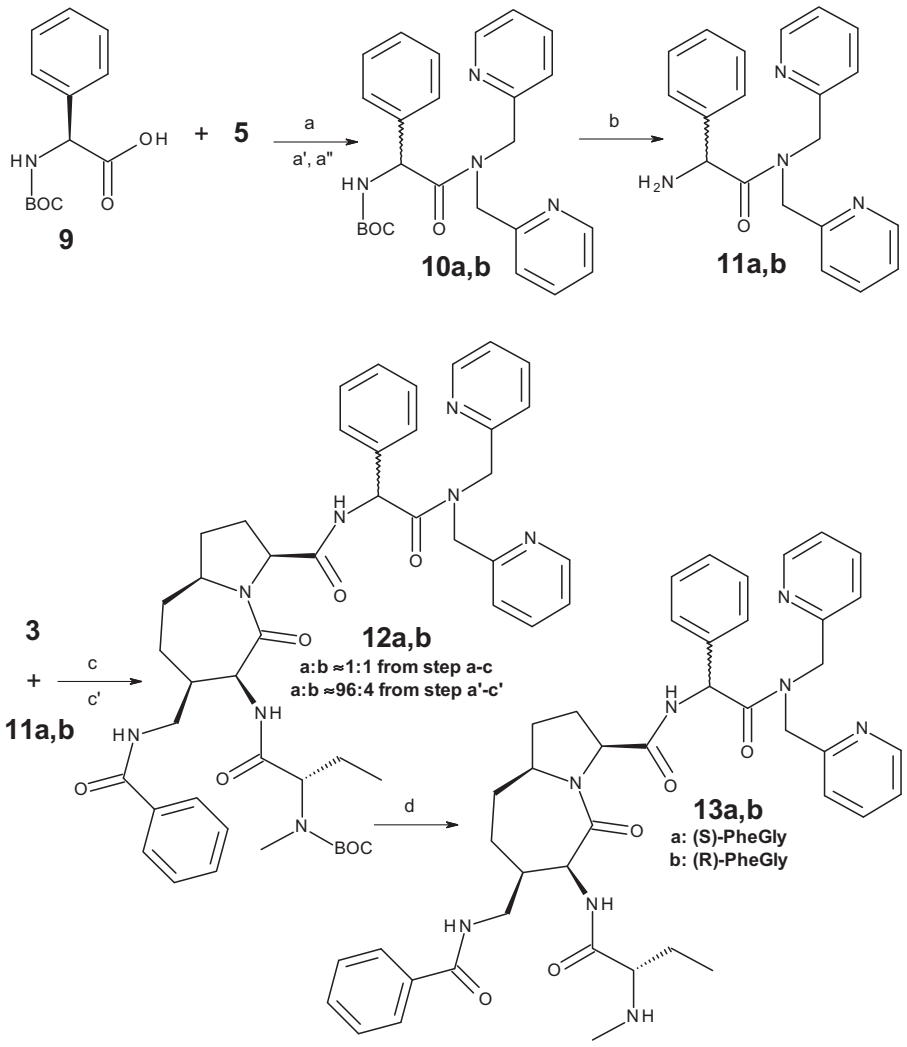

a, TBTU, HOBt, dry DIPEA, dry CH_2Cl_2/DMF 8/1, N_2, rt, **92%**; a', N-Boc-(S)-PheGly, iBuOCOCl, 4-Me-morpholine, dry THF, N_2, -15°C; a", **5**, dry THF, N_2, -30°C, **70%** (2 steps from a'); b, TFA, CH_2Cl_2, 0°C to rt; c, TBTU, HOBt, dry DIPEA, dry DMF, N_2, 0°C to rt, **85%** (2 steps from b); c', HBTU, HOBt, sym-collidine, dry DMF, N_2, 0°C to rt, **85%** (2 steps from b); d, TFA, CH_2Cl_2, 0°C to rt, reverse phase HPLC, **76%**.

Scheme 3. Synthesis of PheGly-DPA amides **13a**,**b**.

We measured the affinity of compounds **1**, **8**, **13a**,**b**, **18a**,**b**, **19** and **20** for the BIR3 domain of XIAP (Table 1), using a fluorescence polarization-based assay.[22]

Compounds either lacking the 10 phenyl substitution (**8**) or bearing the 'wrong' 10 (*R*)-phenyl group (**13b**, **18b**) do not show affinity for XIAP BIR3. Conversely, compounds bearing the 10 (*S*)-phenyl group retain an affinity for XIAP BIR3 either comparable (**13a**, **18a**), or reduced (**20**) with respect to standard compound **1** (Table 1). Thus, the addition of a Zn^{2+} chelating moiety at the 10 position of ABDs does not necessarily impair their Smac mimetic nature. As expected, PAC-1 **19** does not interact with XIAP BIR3.

We examined the Zn^{2+} chelating ability of compounds **5**, **8**, **13a**, **18a** and **20** by measuring changes of their fluorescence spectra in presence of Zn^{2+}. Each compound was titrated with increasing concentrations of Zn^{2+}, and the corresponding spectra were recorded after equilibration (15 min, see Fig. S1 and text, Supporting Information). Increasing [Zn^{2+}] caused a measurable increase of intensity in the fluorescence emission of standard DPA **5** (Fig. S2, Supporting Information). The growth of a 500 nm band in the spectrum of DAC–DPA **18a** (panel A, Fig. S3, Supporting Information) clearly indicated Zn^{2+} complexation.

The lack of a basic bridge nitrogen among the pyridine rings in **8** (Fig. S4, Supporting Information) and **13a** (panel B, Fig. S3, Supporting Information) should prevent Zn^{2+} chelation. Accordingly, fluorescence emission intensity and emission shape in both spectra were unchanged by Zn^{2+}.

The *o*-hydroxy, *m*-allyl, *N*-acyl (*E*)-phenylhydrazone moiety in DAC–PAC-1 **20** caused an increase of Zn^{2+}-dependent fluorescence intensity and UV–visible absorbance (panels C and D, Fig. S3, Supporting Information). The spectroscopic properties of DAC–PAC-1 **20** allow a thorough characterization of free and bound Zn species in terms of fluorescence quantum efficiency and radiative lifetimes (Table S1, Supporting Information).

Thus, DACs containing various Zn^{2+} chelators may be built on the 10-amide group of Smac mimetics, preserving both pro-apoptotic effects when connected with suitable spacers.

We then determined the effects of compounds **1**, **8**, **13a**,**b**, **18a**,**b**, **19** and **20** on apoptosis-connected cellular processes. Western

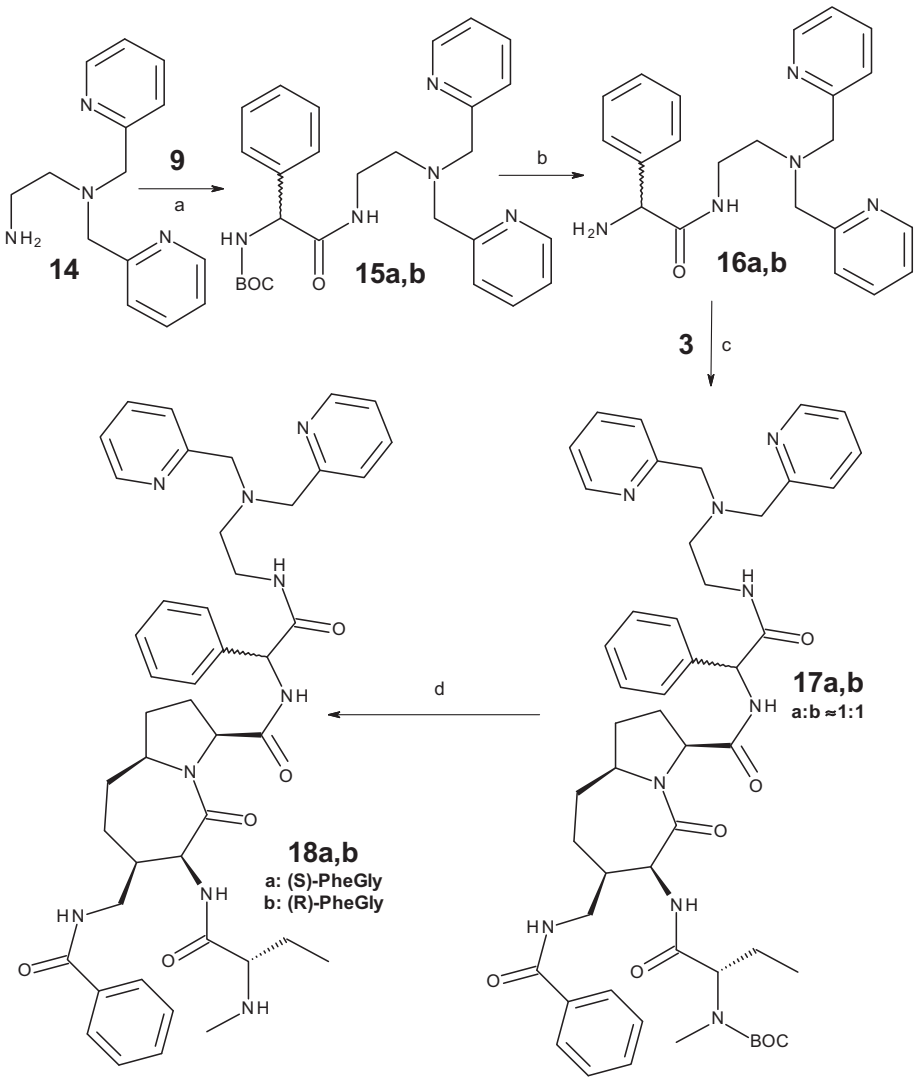

a, TBTU, HOBt, dry DIPEA, dry CH_2Cl_2/DMF 8/1, N_2, rt, **91%**; b, TFA, CH_2Cl_2, 0°C to rt, **98%**; c, TBTU, HOBt, sym-collidine, dry DMF, N_2, 0°C to rt, **86%**; d, TFA, CH_2Cl_2, 0°C to rt, reverse phase HPLC, **64%**.

Scheme 4. Synthesis of Smac mimetic–Zn^{2+} chelating DAC amides **18a**,**b**.

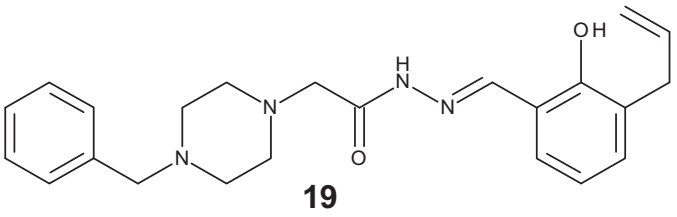

Figure 3. Structure of pro-apoptotic Zn^{2+} chelator **19** (PAC-1).

blots from sensitive (MDA-MB231), partially resistant (BT-549) and fully Smac mimetic-resistant breast carcinoma tumor cell lines (MDA-MB453) are shown in Figures 4, S5 and S6.

Their effects on cIAP1 degradation in Smac mimetic-sensitive MDA-MB231 cells are shown on lane 1, Figure 4. cIAP1 degradation was almost complete for DAC–DPA **18a**, significant for standard **1**, **13a** and DAC–PAC-1 **20**, and negligible for other compounds, in agreement with their affinity for BIR3 XIAP. The activation of apoptosis, quantified through the cleaved forms of caspase-3 (lane 4) and PARP proteins (lane 3), is stronger for standard **1** and DAC–DPA **18a**, significant for **13a** and DAC–PAC **20**, and negligible for other compounds. The levels of XIAP (lane 2, Fig. 4) are less affected by our compounds, excluding a strong Zn^{2+} chelation-mediated effect of DACs **18a** and **20** on XIAP.

Their effects on moderately Smac mimetic-resistant BT-549 cells (Fig. S5, Supporting Information) were weaker in potency, but similar to what observed in MDA-MB231 cells. Standard **1** and DAC–DPA **18a** reduced cIAP1 levels and weakly activated caspase-3 and PARP, while DAC–PAC-1 **20** reduced cIAP1 levels. As to fully Smac mimetic-resistant MDA-MB543 cells (Fig. S6, Supporting Information), compounds **1**, **13a** and DACs **18a** and **20** caused cIAP1 degradation, but did not activate caspase-3 or PARP. The levels of XIAP were not markedly affected in both cell lines.

We then determined the cytotoxicity of compounds **1**, **8**, **13a**,**b**, **18a**,**b**, **19** and **20** on the same cell lines (Table 2) after 24 h exposure.

XIAP-inactive compounds **13b** and **18b** were not cytotoxic against Smac mimetic-sensitive MDA-MB-231 cells. Good cytotoxicity (<5 μM) was observed with standard compounds **1** and **19**, and with DAC–PAC-1 **20**. Surprisingly, nanomolar IAP inhibitors **13a** and DAC–DPA **18a** showed only moderate, >10 μM

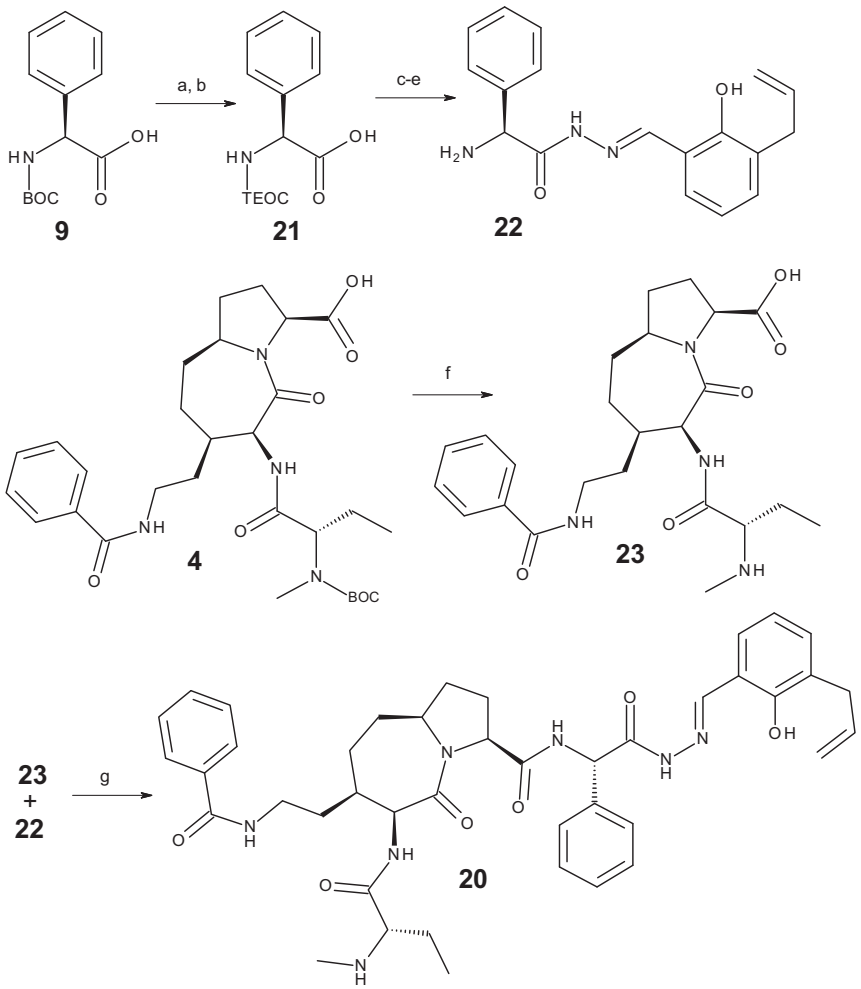

a, TFA, CH_2Cl_2, rt; b, Teoc-OSu, Na_2CO_3, THF/H_2O 2/1, 0°C to rt, **96%** (2 steps); c, $N_2H_4.H_20$, EDC, HOBt, CH_3CN, rt; d, 3-allylsalicylaldehyde, cat. HCl, EtOH, reflux, 49% (2 steps); e, TBAF, THF, 70°C; f, TFA, CH_2Cl_2, rt, **95%**; g, HATU, HOAt, sym collidine, dry DMF, N_2, 0°C to rt, reverse phase HPLC, **63%**.

Scheme 5. Synthesis of Smac mimetic–Zn^{2+} chelating DAC *N*-acylhydrazone **20**.

Table 1
XIAP-BIR3 binding affinity

	IC_{50}, nanomolar
1[6]	260
8	>10,000
13a	370
13b	>10,000
18a	91
18b	>10,000
19	>10,000
20	1090

cytotoxicity. We presume that the tridentate basic nature of DPA-derived Zn^{2+} chelating moieties in **13a** and **18a** severely hindered their permeability through cell membranes.

PAC-1 **19** and DAC–PAC-1 **20** showed cytotoxicity against tumor cell lines partially or totally resistant to Smac mimetics (Table 2). DPA-based **13a** and **18a** were inactive, possibly also due to above mentioned permeability issues. Zn^{2+} chelation by PAC-1 **19** caused cytotoxicity against BT-549 and especially MDA-MB453 cells. The slightly lower cytotoxic effects of DAC–PAC-1 **20** are likely due to stronger *o*-hydroxy, *m*-allyl, *N*-acyl (*E*)-phenylhydrazone-driven Zn^{2+} chelation.

In conclusion, we have prepared pro-apoptotic DACs built by joining a Zn^{2+}-chelating moiety (DPA—**18a**, PAC-1—**20**) with a Smac mimetic through its 10 amide group. DACs mostly preserve the biological activity of both components, but do not appear to

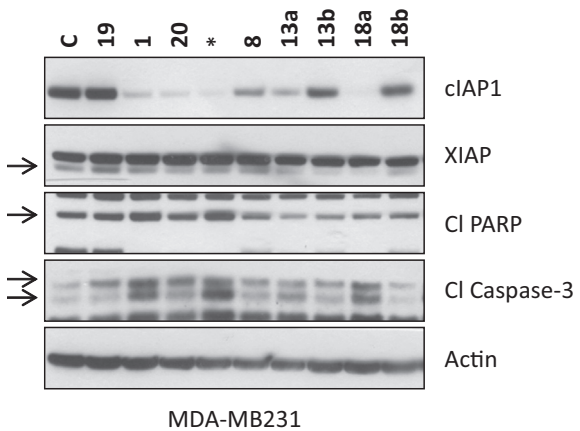

Figure 4. Pro-apoptotic effects of **1**, **8**, **13a**,**b**, **18a**,**b**, **19** and **20** on Smac mimetic-sensitive MDA-MB231 cells. C, control; *, unrelated compound/experiment.

Table 2
Cytotoxicity of compounds **1**, **8**, **13a**,**b**, **18a**,**b**, **19** and **20**

	MDA-MB231*	BT-549*	MDA-MB543*
1	2.3	>25	>25
8	21.0	>25	>25
13a	18.5	>25	>25
13b	>25	>25	>25
18a	16.0	>25	>25
18b	>25	>25	>25
19	4.7	14.3	2.0
20	4.1	21.7	6.2

* IC_{50}, micromolar. Measured by CellTiter-Glo (Promega).

provide synergistic effects in cellular assays. In particular, DPA-based moieties are detrimental to cytotoxicity due to poor permeability through cell membranes.

We plan to continue our investigation on Smac mimetic—Zn^{2+} chelator DACs by exploring their connection through the 4 position of Smac mimetics; by studying the influence of linkers between units; and by employing Zn^{2+} chelating moieties with more suitable physico-chemical properties for cellular permeation. These studies will be reported in due time.

Acknowledgments

We gratefully acknowledge MIUR – Italy (Ministero dell'Università e della Ricerca) for financial support (PRIN project 2010NRREPL: Synthesis and biomedical applications of tumour-targeting peptidomimetics). The use of instrumentation purchased through the Regione Lombardia—Fondazione Cariplo joint project 'SmartMatLab Centre' (decreti 12689/13, 7959/13; Azione 1 e 2) is gratefully acknowledged; A.B. thanks Dr. Marta Penconi for the collection of fluorescence data and discussions.

Supplementary data

Supplementary data (experimental procedures for the synthesis of compounds **3**, **4**, **8**, **13a**, **13b**, **18b** and DACs **18a** and **20**. LC–MS and NMR characterization of compounds **3**, **4**, **8**, **13a**, **13b**, **18a**, **18b** and DACs **18a** and **20**. Experimental procedures for cell-free testing/binding affinity determination of compounds, DACs and standards in presence of BIR3 constructs from XIAP. Experimental procedures for Zn^{2+} titration of compounds **5**, **8**, **13a**, and DACs **18a** and **20**. Experimental procedures for mechanism of action studies and cellular cytotoxicity testing of compounds, DACs and standards against human tumor cell lines) associated with this article can be found, in the online version, at http://dx.doi.org/10.1016/j.bmcl.2016.08.065.

References and notes

1. http://www.phrma.org/media/releases/nearly-1000-medicines-development-help-patients-their-fight-against-cancer.
2. Mauro, M. J. *Hematology* **2006**, *1*, 219.
3. Sangrajrang, S.; Fellou, A. *Chemotherapy* **2000**, *46*, 327.
4. Mingozzi, M.; Manzoni, L.; Arosio, D.; Dal Corso, A.; Manzotti, M.; Innamorati, F.; Pignataro, L.; Lecis, D.; Delia, D.; Seneci, P.; Gennari, C. *Org. Biomol. Chem.* **2014**, *12*, 3288.
5. Manzoni, L.; Belvisi, L.; Arosio, D.; Civera, M.; Pilkington-Miksa, M.; Potenza, D.; Caprini, A.; Araldi, E. M. V.; Monferini, E.; Mancino, M.; Podestà, F.; Scolastico, C. *ChemMedChem* **2009**, *4*, 615.
6. Seneci, P.; Bianchi, A.; Battaglia, C.; Belvisi, L.; Bolognesi, M.; Caprini, A.; Cossu, F.; De Franco, E.; De Matteo, M.; Delia, D.; Drago, C.; Khaled, A.; Lecis, D.; Manzoni, L.; Marizzoni, M.; Mastrangelo, E.; Milani, M.; Motto, I.; Potenza, D.; Rizzo, V.; Servida, F.; Turlizzi, E.; Varrone, M.; Vasile, F.; Scolastico, C. *Bioorg. Med. Chem.* **2009**, *17*, 5834.
7. Hooper, N. M. *Zinc Metalloproteases in Health and Disease*; Taylor & Francis: London, 1996.
8. Truong-Tran, A. Q.; Grosser, D.; Ruffin, R. E.; Murgia, C.; Zalewski, P. D. *Biochem. Pharmacol.* **2003**, *66*, 1459.
9. Makhov, P.; Golovine, K.; Uzzo, R. G.; Rothman, J.; Crispen, P. L.; Shaw, T.; Scoll, B. J.; Kolenko, V. M. *Cell Death Differ.* **2008**, *15*, 1745.
10. Du, C.; Fang, M.; Li, Y.; Wang, X. *Cell* **2000**, *102*, 33.
11. Chai, J.; Du, C.; Wu, J.-W.; Kyin, S.; Wang, X.; Shi, Y. *Nature* **2000**, *406*, 855.
12. Varfolomeev, E.; Blankenship, J. W.; Wayson, S. M.; Fedorova, A. V.; Kayagaki, N.; Garg, P.; Zobel, K.; Dynek, J. N.; Elliott, L. O.; Wallweber, H. J.; Flygare, J. A.; Fairbrother, W. J.; Deshayes, K.; Dixit, V. M.; Vucic, D. *Cell* **2007**, *131*, 669.
13. Sun, H.; Nikolovska-Coleska, Z.; Lu, J.; Meagher, J. L.; Yang, C.- Y.; Qiu, S.; Tomita, Y.; Ueda, Y.; Jiang, S.; Krajewski, K.; Roller, P. P.; Stuckey, J. A.; Wang, S. *J. Am. Chem. Soc.* **2007**, *129*, 15279.
14. Bianchi, A.; Ugazzi, M.; Ferrante, L.; Lecis, D.; Scavullo, C.; Mastrangelo, E.; Seneci, P. *Bioorg. Med. Chem. Lett.* **2012**, *22*, 2204.
15. The detailed, optimized Scheme to compound **4** is reported in the Supplementary Information.
16. Zuo, J.; Schmitt, S. M.; Zhang, Z.; Prakash, J.; Fan, Y.; Bi, C.; Kodanko, J. J.; Dou, Q. P. *J. Cell. Biochem.* **2012**, *113*, 2567.
17. The experimental protocol to compounds **8**, **13b**, **18a**,**b** and **20**, and their analytical characterization are reported in the Supplementary Information.
18. Experimental protocol to DAC–DPA **18a**:
tert-Butyl 2-(bis(pyridin-2-ylmethyl)amino)-2-oxo-1-(S)-phenylethyl carbamate (**10a**): 4-Methylmorpholine (0.168 mL, 1.528 mmol, 3 equiv) was added under nitrogen at −30 °C to a stirred solution of *N*-Boc-(*S*)-PheGly **9** (128 mg, 0.510 mmol, 1 equiv) and $ClCO_2{}^iBu$ (0.09 mL, 0.713 mmol, 1.4 equiv) in 2.4 mL of dry THF. After stirring for 30 min, di(2-picolyl)-amine (DPA, **5**, 152.2 mg, 0.764 mmol, 1.5 equiv) was added at −30 °C to the colourless suspension. The mixture was stirred at −30 °C, and monitored by TLC (eluant condition CH_2Cl_2/MeOH 95:5). After 3 hours, 15 mL of water were added to the mixture. The resulting colourless solution was extracted with AcOEt (2 × 20 mL). The organic phases were washed with NH_4Cl (3 × 20 mL) and with 30 mL of brine. The organic phases were dried with Na_2SO_4, filtered and the solvent was removed under reduced pressure. The crude product (284.1 mg) was purified by reverse phase flash chromatography (eluant H_2O/MeCN from 100:0 to 0:100), yielding 150.1 mg of compound **10a** as a pale yellow oil (0.351 mmol, 69% yield).
2-Amino-2-(S)-phenyl-N,N-bis(pyridin-2-ylmethyl)acetamide (**11a**): TFA (3.48 mmol, 0.265 ml, 30 equiv) was added under stirring at 0 °C to a solution of **10a** (50.0 mg, 0.116 mmol, 1 equiv) in 0.58 mL of CH_2Cl_2 [0.2 M]. The reaction mixture was stirred at 0 °C for 30 min, and at rt for 2 h while monitoring by TLC (eluant CH_2Cl_2/MeOH 95:5). The solvent was removed under reduced pressure. Two aliquots of toluene (2 × 2 mL) were then added, and removed under reduced pressure. The residue was then dried under vacuum yielding 78.3 mg of crude product **11a** as a yellow solid, that was used without further purification.
tert-Butyl (S)-1-((3S,6S,7R,9aS)-7-(benzamidomethyl)-3-(2-(bis(pyridin-2-ylmethyl)amino)-2-oxo-1-phenylethylcarbamoyl)-5-oxooctahydro-1H-pyrrolo[1,2-a]azepin-6-ylamino)-1-oxobutan-2-yl(methyl)carbamate (**12a**): Compound **11a** (58.3 mg, 0.140 mmol, 1.2 equiv) and 2,4,6 trimethylpyridine (0.03 mL, 2 equiv) were dissolved under nitrogen atmosphere in 0.8 mL of anhydrous DMF. The mixture was cooled at 0 °C, then HBTU (57.1 mg, 0.151 mmol, 1.3 equiv) and HOBt (23.5 mg, 0.174 mmol, 1.7 equiv) were added. After 10 min, a solution of compound **3** (78.3 mg, 0.116 mmol, 1 equiv) and *sym*-collidine (0.047 mL, 3 equiv) in 0.4 mL of anhydrous DMF was added, the reaction mixture was warmed up to rt and monitored by TLC (eluant DCM/MeOH 95:5). After 12 h the solution was diluted with 20 mL of AcOEt and washed with NH_4Cl (3 × 20 mL). The organic phases were dried with Na_2SO_4, filtered and the solvent was removed under reduced pressure. The crude product (120.9 mg) was purified by flash chromatography (eluant DCM/MeOH 96:4), yielding 84.7 mg of compound **12a** as a pale yellow solid (0.098 mmol, 85% yield, ≈92 de).
(3S,6S,7R,9aS)-7-(Benzamidomethyl)-N-(2-(bis(pyridin-2-ylmethyl)amino)-2-oxo-1-phenylethyl)-6-((S)-2-(methylamino)butanamido)-5-oxooctahydro-1H-pyrrolo[1,2-a]azepine-3-carboxamide (**13a**): TFA (0.230 mL) was added dropwise over a period of 30 min at 0 °C to a stirred solution of compound **12a** (84.7 mg, 0.098 mmol, 1 equiv) in CH_2Cl_2 (0.5 mL). The reaction mixture was stirred at rt and monitored by TLC (eluant DCM/MeOH 95:5). After 2 hours the solvent was removed under reduced pressure. Two aliquots of toluene (2 × 2 mL) were then added, and removed under reduced pressure. The remaining residue was then dried under vacuum yielding 100.4 mg of crude product as a brown viscous oil. The crude product was purified by HPLC (eluant H_2O/MeCN 100:0 to 0:100), yielding 74.6 mg of compound **13a** as a white solid (0.068 mmol, 71% yield), and 3.2 mg of compound **13b** as a white solid (0.003 mmol).
19. Fukuoka, S.; Kida, T.; Nakajima, Y.; Tsumagari, T.; Watanabe, W.; Inaba, Y.; Mori, A.; Matsumura, T.; Nakano, Y.; Takeshita, K. *Tetrahedron* **2010**, *66*, 1721.
20. Putt, K. S.; Chen, G. W.; Pearson, J. M.; Sandhorst, J. S.; Hoagland, M. S.; Kwon, J.-T.; Hwang, S.-K.; Jin, H.; Churchwell, M. I.; Cho, M.-H.; Doerge, D. R.; Helferich, W. G.; Hergenrother, P. J. *Nat. Chem. Biol.* **2006**, *2*, 543.
21. Peterson, Q. P.; Goode, D. R.; West, D. C.; Ramsey, K. N.; Lee, J. J. Y.; Hergenrother, P. J. *J. Mol. Biol.* **2009**, *388*, 144.
22. Nikolovska-Coleska, Z.; Meagher, J. L.; Jiang, S.; Kawamoto, S. A.; Gao, W.; Yi, H.; Qin, D.; Roller, P. P.; Stuckey, J. A.; Wang, S. *Anal. Biochem.* **2008**, *374*, 87.